Journal of Alloys and Compounds 500 (2010) 129–133

Contents lists available at ScienceDirect

Journal of Alloys and Compounds

journal homepage: www.elsevier.com/locate/jallcom

Microstructural and mechanical properties (hardness) investigations of Al-alloyed ductile cast iron

A. Shayesteh-Zeraati[a], H. Naser-Zoshki[b], A.R. Kiani-Rashid[c,*]

[a] Department of Materials Science and Engineering, Sharif University of Technology, P.O. Box 11365-9466, Azadi Avenue, Tehran, Iran
[b] Department of Materials and Metallurgical Engineering, Iran University of Science and Technology, Tehran, Iran
[c] Department of Materials Engineering, School of Engineering, Ferdowsi University of Mashhad, P.O. Box. 91775-1111, Azadi Square, Mashhad, Khorasan Razavi, Iran

ARTICLE INFO

Article history:
Received 13 January 2010
Received in revised form 31 March 2010
Accepted 1 April 2010
Available online 8 April 2010

Keywords:
Microstructure
Kinetics
X-ray diffraction
Diffusion

ABSTRACT

Microstructures and hardness of aluminum alloy ductile iron were investigated by SEM, XRD, EPMA and hardness measurement techniques. The results show, increasing the Al-alloying element leads to decrease of free ferrite and carbide, as well as increase in the pearlite volume fraction. It is also has been found that in the higher values of Al, about 85% of the matrix would be pearlite. It is indicated that an increase in the aluminum content also leads to a decrease in the spacing between pearlite layers. XRD results show, in the presence of Al, intermetallic compounds such as Al_6Fe, $AlFe_3C_{0.5}$, Fe_3Al and FeAl were produced. Furthermore the hardness measurements illustrate that by increasing the Al content, the microhardness of ferrite and pearlite and specimens hardness have been significantly increased.

1. Introduction

In comparison with the other types of cast iron, ductile iron has higher strength, appropriate toughness, good machinability, fair wear resistance, high molten fluidity and low melting point. Its major advantage is good strength and flexibility, besides the high elastic modulus. In fact, the spherical shape for graphite causes unique properties in this class of irons. The final microstructure of as-cast ductile iron has been significantly controlled by melting process, chemical composition and cooling rate [1].

The as-cast microstructure is governed by the solidification process and solid state transformation (eutectoid reaction). The inoculation practice and the cooling rate control the nodule count, while the matrix microstructure depends on the conditions under which the eutectoid reaction occurs. Among the variables that influence the mechanism of the eutectoid reaction are the chemical composition and the cooling rate through the eutectoid temperature range. The result of eutectoid transformation have key role in determining the cast iron mechanical properties. Thus, the effect of alloying elements on mechanical properties of ductile iron might be related to their influence on eutectoid transformation [2–4].

The investigation of eutectoid transformation in cast irons is more difficult than steels. In steel, the meta-stable transformation of Austenite to ferrite and cementite happen, while in cast iron, eutectoid transformation is comprised both stable reaction which lead to formation of ferrite and graphite, as well as meta-stable reaction that result is pearlite formation [2–5]. Since the eutectoid transformation in cast irons is performed by a competitive process between meta-stable and stable transformations, it is important to study the growth kinetic of both transformations that were mentioned [4].

Alloying elements take significant effects in eutectic transformation by changing the eutectic stability and instability temperatures. Among the alloying elements, Al promotes the graphite formation during the eutectic transformation. On the other hand, it stabilizes the pearlite in the eutectoid transformation. Aluminum, similarly to Si, is dissolved in ferrite and austenite at high values, whereas its solubility in carbide is low [6–9]. It has been described that Al acts as an inoculant and refiner in grey cast iron and increases the number of eutectic cells. It was reported that Al addition favor tendencies for graphite nucleation in cast irons [10].

The volume fraction of pearlite amount in Fe–C–Al iron matrix is significantly more in comparison to Fe–C–Si iron; the former system shows more tendencies to coring [11–13].

Although many of researchers investigated the microstructural changes of Al-alloy ductile iron, there is no comprehensive study about kinetically factors such as diffusion rate and Al distribution in matrix. In this paper, a more comprehensive investigation on microstructural transformation by means of SEM, XRD and EPMA

* Corresponding author. Tel.: +98 511 7683199; fax: +98 511 8763305.
E-mail addresses: alishayesteh63@gmail.com, alishayesteh63@yahoo.com (A. Shayesteh-Zeraati), h.naserzoshki@gmail.com, hamedenaser@yahoo.com (H. Naser-Zoshki), kianirashid@gmail.com, fkiana@yahoo.com (A.R. Kiani-Rashid).

0925-8388/$ – see front matter © 2010 Elsevier B.V. All rights reserved.
doi:10.1016/j.jallcom.2010.04.003

Table 1
Chemical composition of ductile cast iron samples containing Al (weight percent).

Alloy	C	Al	Si	Ni	Mn	P	S	Mg	Fe
0.48% Al	3.68	0.48	1.06	0.03	0.06	<0.005	<0.005	<0.05	Balance
4.88% Al	3.44	4.88	1.22	0.05	0.10	<0.005	<0.005	<0.05	Balance
6.16% Al	3.25	6.16	1.25	0.07	0.10	<0.005	<0.005	<0.06	Balance

and hardness test for specimens with different Al contents has been carried out. Finally, a new type of this cast iron grade has been developed.

2. Experimental procedure

2.1. Melting

For preparation of spherical cast irons with different percentages of aluminum, we first utilized a Morgan gas-fired furnace (with 25 kg capacity lift-out crucible) and a high-frequency melting plant of 20 kg capacity (with a tilting crucible) for the melting and alloying process. After that, the temperature of the melt increases to 1550 °C; in order to prevent floating and oxidation of aluminum, some small parts of aluminum were added to the bottom section of the melt. Enough time was given to dissolve the aluminum completely in the molten metal. Following aluminum treatment, FeSiMg (5 wt.% Mg) alloy was plunged into the melt iron and ejection of molten metal during solution of magnesium prevented by use of special enclosed reaction vessels. Finally, post-inoculation of ferro-silicon containing 75 wt.% Si was carried out in the crucible. As we aimed at adding reaction materials gradually and steadily to the melt, a reaction chamber was designed below the sprue system to hold the inoculants and nodularizers and also to provide better conditions for their reaction with the melt [14].

Finally, according to ASTM A897 M-90, the samples were prepared by sand mold casting and permanent mold casting. After sectioning and polishing the samples, Quantitative measurements of the carbon content in the experimental irons were made using equipment at Swinden Technology Centre of Corus Group PLC (formerly British Steel Ltd.). In order to analyses for aluminum in high Al content ductile irons, an atomic absorption spectrophotometry (AAS) method was used by Hi Search Technology (HIST) of Birmingham University (Table 1).

2.2. Sample preparation

For studying samples microstructures, they were sectioned in proper size and polished by 80-1200 grinding paper. First samples were polished with diamond powders with 1 μm diameter and then the process continued with Al_2O_3 with 0.3 and 0.05 μm diameters. Phase identification was achieved after etching in 2% nital. The same techniques were used to prepare the specimens for hardness measurement.

2.3. Microstructural examination

Optical microscopy (Olympus BX60MF5) equipped with digital camera (JVC 10215670) and SEM (Leo 1450VP) were used to examine and delineate any variations in the microstructure, with changes in the content of Al. For characterizing of microstructure by SEM, a working distance between 12 and 18 mm was chosen, as well as an accelerating voltage of 20 kV. Also, image analysis was performed by Clemex Vision 3.5 system.

The XRD analysis was carried out using Cu Kα target radiation. An automated Philips ADP 1700 diffractometer, operated at 40 kV and 20 mA over 2θ values ranging from 5° to 85°, was used in order to detect the reflection of interest.

Moreover, microanalysis investigations were performed using EPMA CAMECA SX-50 equipped with WDS and EDS, to determine the distribution of Si and Al in the samples during solidification. This instrument has also all of the automatic abilities to quantitative analysis and due to its suitable software; data were reported in form of a map or series of points.

2.4. Hardness measurements

Microhardness measurements were made using a Vickers Engineering Group Vickers hardness machine at a load of 25 g on polished samples and Hardness of specimen measured by Universal Koopa machine at a load of 150 kg. A mean of five measurements was made for each sample.

3. Results and discussion

The microstructure of the sand mold specimens obtained by LOM is shown in Fig. 1. Fig. 1a shows the structure of the sample containing 0.48% Al. This sample consists of spherical graphites distributed randomly in the ferrite–pearlite matrix which is the conventional structure of this type of cast irons. Generally, an increase in the Al content, leads to a reduction in the volume fraction of ferrite and the pearlite volume fraction is increased. The microstructure of the sample containing 6.16% Al is shown in Fig. 1b. As it can be seen, the major part of the carbides in pearlite is spheriodized.

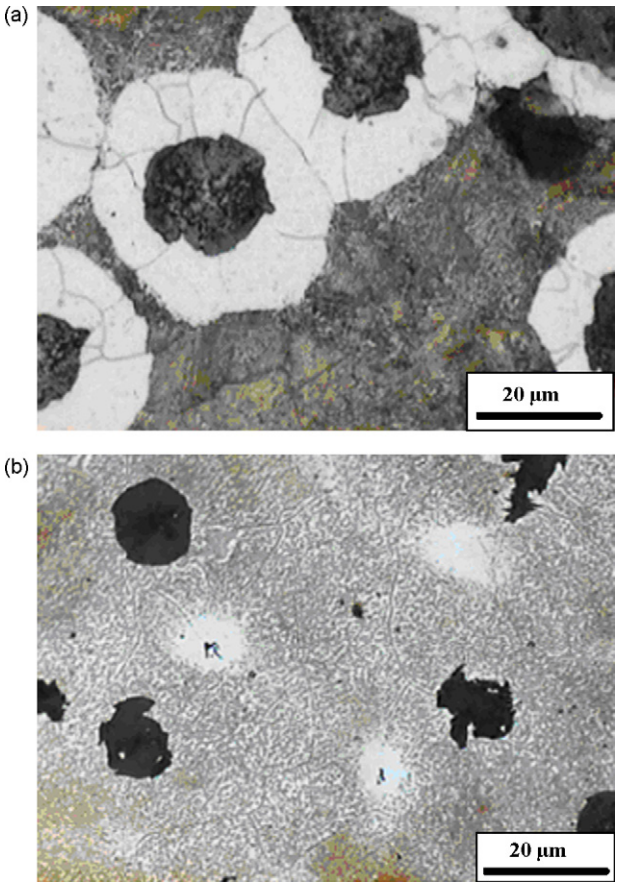

Fig. 1. The LOM micrographs of sand mold poured cast iron with: (a) 0.48% Al and (b) 6.16% Al.

Fig. 2 illustrates the SEM images of the samples containing 0.48%, 4.88% and 6.16% Al which solidified in the permanent mold. We can observe that as Al content increases, the pearlite become finer and carbides are significantly removed from the matrix.

The volume fraction of the phases in the structure is reported in Table 2. The results reveal that as the aluminum content increases, free ferrite volume is reduced and the matrix exhibit more volume fraction of pearlite.

Alloying elements that dissolve in liquid and solid iron phases change the equilibrium temperature in Fe–C phase diagram. In general, the elements increasing the interval between eutectic stability and instability temperature, promote graphite formation while the elements decreasing this interval, promote carbide formation [9]. Al increases the interval between eutectic stability and instability temperature, so the formation of carbide becomes difficult. Table 3 illustrates the temperature intervals between stability and instability for the studied cast iron samples (see Appendix A). Table 3

Table 2
Microstructural characteristics of samples solidified in permanent mold.

Alloy	Pearlite (%)	Ferrite (%)	Carbide (%)	Graphite (%)
0.48% Al	72.2	15.5	4.5	7.8
4.88% Al	74.2	18.4	–	7.4
6.16% Al	87.2	6	–	6.8

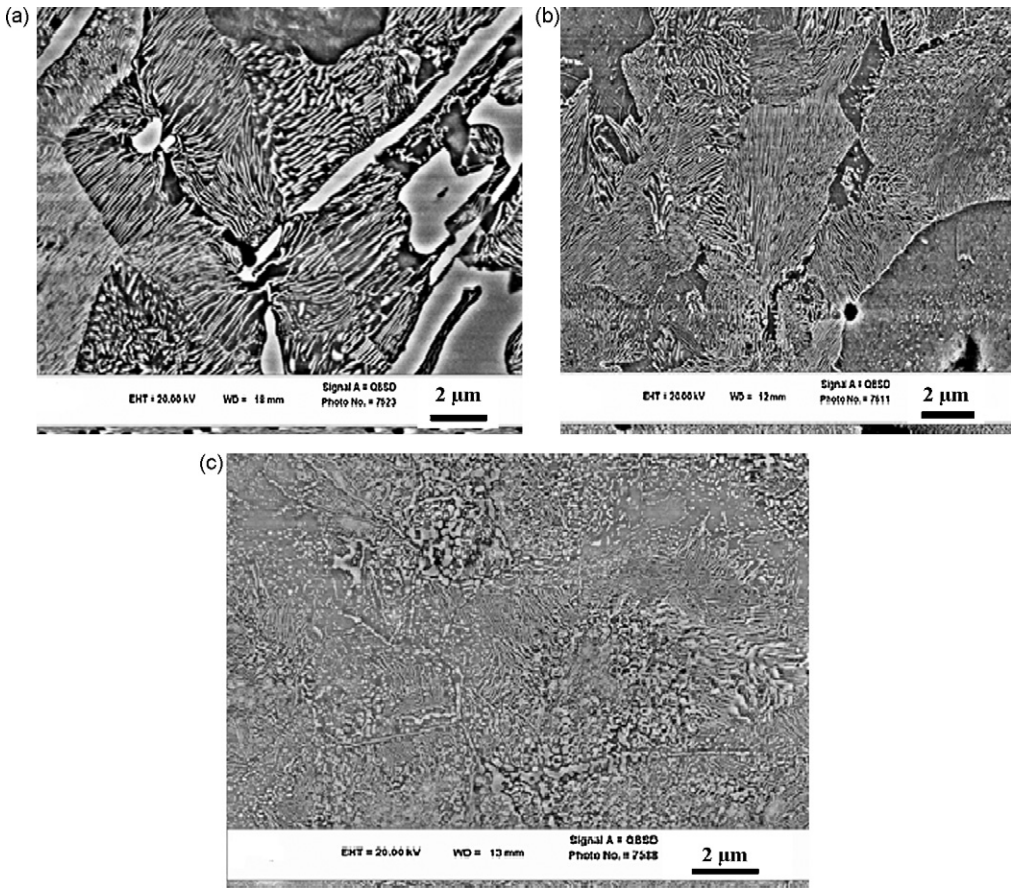

Fig. 2. SEM images of permanent mold poured irons with: (a) 0.48% Al, (b) 4.88% Al and (c) 6.16% Al.

shows that this interval is considerably increased with increasing the Al content and this leads to a lower carbide formation. Furthermore, the temperature of carbide formation is lower than that of graphite. Raising the eutectic temperature in the presence of Al, the diffusion rate of carbon is increased, so the probability of carbide formation is considerably decreased [8].

In the presence of inoculants, the graphite can be grown without significant under-cooling. Therefore, the solidification can be terminated above the carbide formation temperature. Enhancement of the nucleation sites, as a result of inoculant addition, results in the increase in the number of spherical graphites. So the carbon diffusion paths will be shortened therefore the carbide formation will probably be decrease. In Fe–C–Si–Al system, aluminum and its nitrides, oxides and carbides can be used as inoculants [14,15].

According to the literature, the amounts of graphite nodules in Al-containing ductile iron are higher than conventional ones [12,13]. The higher number of graphite nodules indicates the high graphitizing ability of Al. The diffusion rate of carbon in Al-containing cast iron is different from Si containing. It is accepted that in Al ductile iron, the spherical graphites form at higher temperatures in comparison with Si ductile iron; therefore Al considerably increases the diffusion rate of C in molten metal. According to the above descriptions we can justify the lower amounts of eutectic carbides in Al-containing ductile irons.

On the other hand, Table 2 shows that Al acts as a pearlite stabilizer during the eutectic transformation. As a result, the increase in the amount of Al increases the volume fraction of pearlite and decreases the volume fraction of ferrite. EPMA image shows high concentration of Al around the graphites (Fig. 3). Al at these regions acts as a diffusional barrier and prevents the diffusion of carbon into the graphite. By limiting the carbon diffusion to the graphite, the feasibility of ferrite formation, which needs to carbon diffusion, is decreased. As a result, formation of pearlite, that has more carbide content, is promoted.

In the presence of Al, finer structure is obtained [11]. On the other hand, austenite grain boundaries are the preferential sites for pearlite nucleation [2]. Thus, enhancement of the Al content provides more sites for pearlite nucleation which results in more pearlite with finer grains morphology.

Johnson and Kovacs [2] have shown that the transformation of austenite to ferrite and graphite begins around graphite regions and continues. Nakae et al. [16], on the other hand, shows that during the solidification the size of austenitic shell around the graphite is fourfold larger than graphite size. Then, by decrease in size of nodular graphite, due to increase of Al content, the size of austenitic shell which surrounds the graphite will be decreased. This will result in decreasing the prone sites for this transformation therefore free ferrite formation process is disrupted. By deferring this transformation, pearlite formation becomes easier and its fraction increases.

The nature of pearlite and ferrite formation reactions is cooperative and diffusional respectively, it is clear that the cooperative

Table 3
Stable and unstable temperatures and their difference for various samples.

Alloy	T_{St}[a]	T_{met}[a]	$\Delta T^a = T_{St} - T_{met}$	$\Delta T^b = T_{St} - T_{met}$
0.48% Al	1162.02	1124.99	37.03	10
4.88% Al	1197.82	1056.65	141.17	98
6.16% Al	1208.24	1036.91	171.33	125

[a] Ref. [9].
[b] Ref. [6].

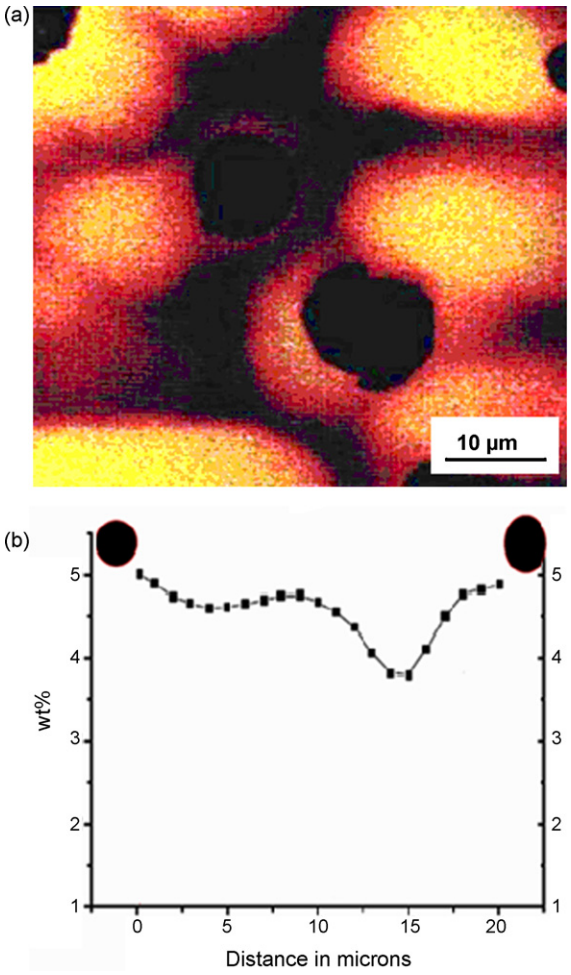

Fig. 3. (a) EPMA maps for 4.88% Al-containing ductile iron and (b) variation of Al distribution between two nodules of graphite.

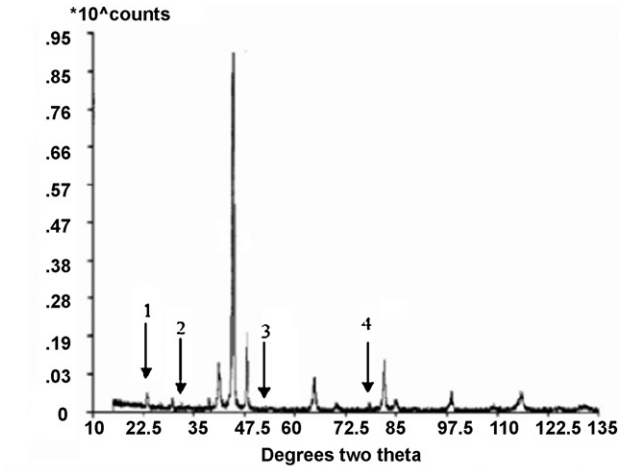

Symbol	Degree Two Theta	Phase
1	23.54, 33.55,41.153, 66.02, 70.75	Al $Fe_3C_{0.5}$
2	17.95, 38.68, 42.32	Fe Al_6
3	30.73, 54.76,113.67	FeAl
4	50.93, 26.72, 63.78, 81.19, 97.65	Fe_3Al

Fig. 4. XRD pattern of 6.16% Al-containing specimen.

reactions predominate against diffusional [4]. As a result of providing suitable nucleation condition for pearlite and decreasing the proper sites for transformation of austenite to ferrite as well as its progressive conditions, enhances the transformation rate of austenite to pearlite.

Comparison of Figs. 1a and 2a shows that in these samples with identical composition, there is no carbides in sand mold cooled samples. Whenever cooling rate is higher than carbon diffusion rate in austenite, molten alloy reaches to instability temperature of eutectic and residual liquid will be solidified in form of carbide, which might be partly decomposed at last. This explanation indicates the influence of effective factor on formation of different structures for identical compositions and different cooling rates (Figs. 1a and 2a).

The hardness and microhardness values of the samples and phases are summarized in Table 4. From the table, it can be seen that as Al content increases, the hardness of the sample is enhanced. Furthermore, it can be observed that the microhardness of the phases is increased. The microhardness of ferrite is unexpectedly higher than the conventional values.

Mechanical properties of cast iron are directly dependent on its microstructure. Mechanical properties are affected by several factors such as, shape and size of nodular graphite, ferrite to pearlite volume ratio, morphology and finesse of the phases as well as segregation and grain boundary features. In this research XRD patterns were used to interpret the results. Fig. 4 shows a XRD pattern of the sample with 6.16% Al. In addition to main phases of microstructure such as α-ferrite and Fe_3C, other Al-containing compounds were found.

Maximum peak of each compound has been marked in the figure and complementary results are given in the table that is shown in the bottom of Fig. 4. Formation of hard and intermetallic compounds such as, Al_6Fe, $AlFe_3C_{0.5}$, Fe_3Al and FeAl has led to promotion of the hardness of solution to higher values than normal ferrite. On the other hand, by increasing the Al content, these peaks intensity increases which might be due to the increased amount of these phases. Also, by enhancement of the Al content, austenitic shell which surrounds graphite becomes smaller and as a result, ferrite with smaller grains and greater hardness will be produced.

Average thickness of pearlite layers is reported in Table 5. These values show that the thickness of pearlite layer is decreased by increasing the Al content. Increasing the hardness of ferrite in the pearlite is due to production of Al–Fe solid solution and refining of the cementite layers in pearlite leads to the increase of microhardness of pearlite in higher Al contents.

By raising the Al content, overall structure becomes finer [6,11]. The increased hardness of samples due to the increasing Al content can be attributed to refining of structure, increasing the pearlite

Table 4
Hardness and microhardness of solidified cast iron samples in permanent mold.

Alloy	Hardness HV (150 kg)	Microhardness (ferrite)	Microhardness (pearlite)
0.48% Al	305	157	301
4.88% Al	377	230	350
6.16% Al	411	274	362

Table 5
Average thickness of pearlite layers.

Alloy	Average layer thickness of pearlite (μm)
0.48% Al	0.257
4.88% Al	0.159
6.16% Al	0.113

volume in structure and enhancement of microhardness of ferrite and pearlite.

4. Conclusions

In this study cast iron samples with different Al contents were cast and their microstructure and hardness have been studied. The results show that the structure of these samples consists of nodular graphite which is distributed randomly in the ferritic–pearlitic matrix. Microstructure observations and more detailed chemical analysis show:

- Increasing the Al content decreases the free ferrite volume as well as increases the pearlite in the matrix.
- The increase of Al content results in a finer structure, especially pearlite, and a decrease in the amount of free carbides.
- By increasing the Al content to higher values, more intermetallic compounds were produced.

Also, hardness and microhardness measurements show:

- The microhardness of ferrite and pearlite phases was increased by raising the Al content.
- High Al-containing samples have higher hardness.

Acknowledgments

Major part of microstructural investigations of present study has been performed in metallography and central laboratory of Ferdowsi University of Mashhad. The authors thank Mr. M.R. Yousef-Sani and Mrs. Sadeghian for metallographic investigations. They also thank Professor D.V. Edmonds and Professor Kandlif (Material Department of University of Leeds) for their valuable support for casting the samples and EPMA and XRD data acquisitions.

Appendix A. Eutectic stability and instability temperatures

In the presence of graphitizing elements, the difference between stable and unstable eutectic temperatures increases, thus the formation conditions of graphite will be improved. The alloying elements, which increase this difference, are known as graphitizing elements. Eqs. (1) and (2) give the stable and unstable eutectic temperatures, respectively [9].

$$T_{St} = 1154\,^{\circ}C + 4(\%Si) + 4(\%Ni) + 8(\%Al) - 2(\%Mn) - 2(\%Mg) \quad (1)$$

$$T_{met} = 1148\,^{\circ}C - 15(\%Si) - 6(\%Ni) - 15(\%Al) + 3(\%Mn) + 3(\%Mg) \quad (2)$$

Addition of aluminum to the cast iron causes a boost in the temperature of eutectic transformation and the distance between stable and unstable solidification lines. This fact promotes the formation of graphite and retards the formation of carbide eutectic. Increase in the eutectic transformation temperature, increases the rate of carbon diffusion in the melt. Using Eqs. (1) and (2) stable and unstable temperatures as well as their difference, are calculated and reported in Table 5. As it can be seen in the table, for samples with 4.88% of aluminum, the difference between stable and unstable temperatures is about 140 °C.

References

[1] J.R. Dave, ASM Specialty Handbook, Cast Iron, ASM Press, 1996.
[2] W.C. Johnson, B.V. Kovacs, The effect of additives on the eutectoid transformation of ductile iron, Metallurgical Transactions A 9A (1978) 219–229.
[3] M.M. Haque, Investigation on properties and microstructures of spheroidal graphite Fe–C–2Si and Fe–C–2Al cast irons, Journal of Materials Processing Technology 191 (2007) 360–363.
[4] F.R. Salazar, M. Herrera-Trejo, M. Castro, N.J. Méndez, T.J. Torres, N.M. Méndez, Effect of nodule count and cooling rate on as-cast matrix of a Cu–Mo spheroidal graphite, JMEPEG 8 (1999) 325–329.
[5] M. Wessen, I.L. Svensson, Modeling of ferrite growth in nodular cast iron, Metallurgical and Material Transactions A 27A (1996) 2209–2220.
[6] S.K. Yu, C.R. Loper, Effect of molybdenum, copper and nickel on the pearlitic and martensitic hardenability of ductile iron, AFS Transaction 96 (1988) 811–821.
[7] A.R. Kiani-Rashid, The influence of aluminum and heat treatment conditions on austempered ductile irons, Ph.D. Thesis, University of Leeds, 2000.
[8] S.M.A. Boutorabi, The austempering kinetics, microstructure and mechanical properties of spheroidal graphite unalloyed aluminium cast iron, Ph.D. Thesis, University of Birmingham, May 1991.
[9] D.M. Stefanescu, Thermodynamic Properties of Iron-Base Alloys, vol. 15, ASM Handbook, 9th edition, Metals Handbook, 1992, pp. 61–70.
[10] R.J. Smickley, K.B. Rundman, The effect of aluminium on the structure and properties of grey cast iron, AFS Transactions 89 (1981) 205–214.
[11] M. Ghoreshy, V. Kondic, Structure and mechanical and casting properties of Fe–C–Al cast iron, Solidification Technology in the Foundry and Cast House, Metal Society (1983) 562–568.
[12] A.R. Kiani Rashid, D.V. Edmonds, Graphite phase formation in Al-alloy ductile iron, IJE Transaction B 15 (3) (2002) 261–272.
[13] A.R. Kiani-Rashid, M.A. Golozar, Microscopic segregation pattern of Al and Si in matrix microstructure of cast irons with spherical graphite, Esteghlal Journal 2 (2003) 177–188.
[14] J.R. Brown, Foseco Ferrous Foundryman's Handbook, Butterworth-Heinemann, 2000, pp. 70–89.
[15] AFS Ductile Iron Hand Book, Cast Metals Institute, 1992.
[16] H. Nakae, S. Jung, H.C. Shin, Formation mechanism of chunky graphite and its preventive measures, Journal of Materials Science and Technology 24 (3) (2008) 289–295.